

# A Novel Organic-Inorganic Hybrid Iron-bipyridyl Keggin Polyoxometalates: Synthesis and Characterization

Rajarshi Chatterjee\*

\*Assistant Professor, Department of Chemistry, A.B.N. Seal College, Coochbehar-736101, West Bengal

Email: rajuchacha.2009@gmail.com

## Abstract

Hybrid organic-inorganic materials are pulling major attention due to their potential to generate unusual structures and properties by combining the features of the organic and inorganic components. Among them, hybrid materials containing polyoxometalates (POMs) have shown fascinating electronic, optical, magnetic and catalytic properties. However, little work has been done on the synthesis of hybrid organic-inorganic materials containing POMs and iron complexes. Transition metal complexes such as iron (II) polypyridyl complexes have been extensively studied for their applications as photo luminescent compounds and sensitizers in the interconversion of light and chemical energy. Particularly, the tris-(2,2'-bipyridine) iron(II) complex  $[\text{Fe}(2,2'\text{-bipy})_3]^{2+}$  is the most widely studied transition metal complex which is capable of splitting water under visible light. In this research, the objective is to study the combination of iron polypyridyl complexes and Keggin polyoxometalate anions through different ways such as coordination bonds, hydrogen bonds and ionic bonds to form hybrid organic-inorganic solids.

## Keywords

*Polyoxometalates, Solvothermal synthesis, Organic-inorganic hybrid*

## Introduction

Hybrid organic-inorganic materials are prepared by combining organic and inorganic building blocks [1]. They are attracting increasing interest as a creative alternative for obtaining new materials with tailored structures and properties [2]. These new hybrid materials have a large variety of applications such as sensors, selective membranes, all sorts of electrochemical devices, from actuators to batteries or super capacitors, supported catalysts or photo electrochemical energy conversion cells [3-4]. Here polyoxometalate is the inorganic fragment of organic-inorganic hybrid POM. Derivatization of POMs with organic partners, including synthetic molecules via covalent bonding as well as electrostatic interaction is expected to result in a synergetic effect and endow novel functions to the POM hybrid [5]. Moreover, the conjugation of an organic ligand onto the POMs offers additional advantages, such as better stability and desirable ligand orientation [6]. It is well known that polyoxometalates (POMs) are early-transition metal oxygen anion clusters of well-defined structure and distinct sizes. Intriguingly, many elements could be easily incorporated in to the

POM frameworks, giving rise to fascinating structural versatility and rich properties. It is therefore not surprising that POMs have broad applications in various fields including material science. The most noticeable advantage of inorganic-organic hybrid POM is that they can favorably combine the often dissimilar properties of organic and inorganic components in one material. In addition, their biphasic structures lead to create multifunctional materials. For example, inorganic clusters or nanoparticles with specific optical, electronic or magnetic properties can be incorporated in organic polymer matrices [7]. The properties of hybrid materials are not only the sum of the individual contributions of both phases, but the role of their inner interfaces could be predominant [8]. The nature of the bonds between organic and inorganic phases has been used to divide into two distinct classes. In Class I, organic and inorganic components are embedded by weak interphase bonding. Only electrostatic interactions, hydrogen bonds, or van der Waals interactions are involved. In Class II materials, the organic and inorganic moieties are linked together through strong chemical covalent or ionic-covalent bonds [9]. The major challenge to synthesize organic-inorganic hybrid materials is to keep or enhance the best properties of each of the components while eliminating or reducing their particular limitations. Recently, ruthenium heterocyclic ligand complex-based building blocks have been used for the synthesis of hybrid organic-inorganic solids through the self-assembly. We are interested in the hydrothermal synthesis of iron-polypyridyl complexes and Keggin polyoxometalate anions through different ways such as coordination bonds, hydrogen bonds and ionic bonds to form hybrid organic-inorganic solids. We did choose iron as it is like ruthenium, one of the congeners of same  $d^6$  family. Many procedures can be foreseen to fabricate POM-based hybrid materials, but solvothermal synthesis of hybrid POM is a novel method till date. Here, we report novel hybrid organic-inorganic compound  $[\text{Fe}(2,2'\text{-bipy})_3]_2[\text{SiW}_{12}\text{O}_{40}]$  which is synthesized under hydrothermal reaction method. The complex is characterized by elemental analysis, UV-vis spectroscopy, thermogravimetric analysis, IR spectroscopy and Single crystal X-ray diffraction.

## Experimental

### Materials and methods

Sodium nonatungstosilicate,  $\text{Na}_{10}[\alpha\text{-SiW}_9\text{O}_{34}]$ , was prepared according to the reported method [10] and was recrystallized three times from triply distilled water before use. Chemicals were readily available from commercial sources and were used as received without further purification.  $\text{FeCl}_2$  (AR Loba, India), 2,2'-bipyridine (Merck, India), and  $\text{H}_2\text{SO}_4$  (Merck, India) were of reagent grade and used as received. Deionized water was used as the solvent.

### Synthesis of tris-(2,2'-bipyridyl) iron(II) silicotungstate $[\text{Fe}(2,2'\text{-bipy})_3]_2[\text{SiW}_{12}\text{O}_{40}]$

The complex was synthesized hydrothermally from a mixture of ferrous chloride  $\text{FeCl}_2$ , 2,2'-bipyridine powder,  $\text{Na}_{10}[\alpha\text{-SiW}_9\text{O}_{34}]$  and de-ionized water. The pH of the resulting mixture was adjusted with 0.5 mL of 1M  $\text{H}_2\text{SO}_4$  to approximately 2. As expected, control of the pH of the reaction mixture is critical for the crystallization of compound 1. It can be crystallized in a narrow pH at around 2 and in a temperature range of 130-150°C. The detailed procedure is as follows:  $\text{Na}_{10}[\alpha\text{-SiW}_9\text{O}_{34}]$  (0.614 g, 0.25 mmol) was dissolved in hot water (20 ml). Then solid  $\text{FeCl}_2$  (0.158 g, 1.25 mmol) was added to the solution. The mixture was heated with stirring for 30 minutes. 2,2'-Bipy (0.078 g, 0.5 mmol) was then added with constant stirring. The resulting solution was stirred at 80°C for another 30 minutes. The mixture was then transferred with subsequent pH adjustment into a Teflon jacket stainless steel pressure vessel and kept in an oven at 160°C for 5 days under autogenous pressure. The solution was cooled by decreasing the temperature at a

regular interval of 5°C over 1 day. The resulting dark red rhombic crystals of  $[\text{Fe}(2,2'\text{-bipy})_3]_2[\text{SiW}_{12}\text{O}_{40}]$  were filtered off, washed with water, and dried at room temperature. Yield: 55% (based on Fe). Elemental analysis: calculated for  $\text{C}_{60}\text{H}_{48}\text{N}_{12}\text{O}_{40}\text{Fe}_2\text{SiW}_{12}$ : C, 17.95; H, 1.21; N, 4.19; found: C, 16.85; H, 1.03; N, 3.73%.

### Physical measurements

The composition of the starting material ( $\text{Na}_{10}[\alpha\text{-SiW}_9\text{O}_{34}]$ ) and the final polyoxo product  $[\text{Fe}(2,2'\text{-bipy})_3]_2[\text{SiW}_{12}\text{O}_{40}]$  with respect to the atom% of W and Si were estimated by SEM-EDX method and found to be 9:1 and 12:1 respectively. Elemental analyses were carried out using a Perkin–Elmer 240 elemental analyzer. Spectral measurements were made in a Varian Cary 1E UV-visible spectrophotometer with 1.00 cm glass cells. IR (400–4000  $\text{cm}^{-1}$ ) was recorded in KBr pellets on a Nicolet Magna IR 750 series-II FTIR spectrophotometer.

### Crystal data collection and refinement

For better structural elucidation, both powder and single crystal XRD were done. Powder XRD patterns were obtained by Bruker D8 advance diffractometer with monochromatic  $\text{CuK}\alpha$  ( $\lambda = 1.5418 \text{ \AA}$ ) with step size of  $0.02^\circ \text{ s}^{-1}$ , whereas X-ray diffraction data for compound 1 were collected on a Bruker Kappa Apex II CCD diffractometer with graphite monochromated  $\text{Mo K}\alpha$  radiation ( $\lambda=0.71073\text{\AA}$ ) at 293 K. The structures were solved by the direct methods and refined by full-matrix least squares on F2 using the SHELXTL-97 software. The hydrogen atoms were treated as riding on their parent carbon atoms with  $d(\text{C-H})= 0.93\text{-}0.95\text{\AA}$  and  $U_{\text{iso}}= 1.2U_{\text{eq}}(\text{C})$ . All the non-hydrogen atoms were refined anisotropically. A summary of crystal data and relevant refinement parameters for complex 1 are given below in Table 1 and selected bond distances are given in Table 2. Molecular graphics were prepared with the aid of WinGx [11] packages.

**Table 1: crystal data and relevant refinement parameters**

| Crystal Data and details of structure refinements for complex 1. |   |
|--|---|
| Empirical formula  | $\text{C}_{30}\text{H}_{24}\text{FeN}_6\text{O}_{20}\text{Si}_{0.50}\text{W}_6$ (1) |
| Formula weight   | 1960  |
| Crystal system   | Triclinic   |
| Space group  | $P\bar{1}$ (2)  |
| a, b, c (Å)  | 13.160(14), 14.750(16), 21.85(2)  |
| $\alpha, \beta, \gamma$ (°)                                      | 90, 94.269(10), 90  |
| Volume (Å <sup>3</sup> )   | 4230(8)   |
| Z  | 4   |
| Density (calculated) $\text{Mg/m}^3$                             | 3.079   |
| Absorption coefficient $\text{mm}^{-1}$                          | 16.6  |
| No of observed data  | 23196   |
| Independent reflections  | 7775 [ $R_{\text{int}}=0.088$ ]   |
| Data / restraints / parameters                                   | 7775/ 0/592   |
| Goodness-of-fit on $F^2$   | 1.190   |
| Final R indices [ $ I > 2\sigma(I) $ ]                           | $R_1=0.0706$ , $wR_2 = 0.1512$  |
| Final R indices (all data)                                       | $R_1=0.0865$ , $wR_2 = 0.1583$  |
| Largest diff peak and hole ( $e.\text{\AA}^{-3}$ )               | 2.034 and $-3.662$  |

Compound 1 crystallizes in the triclinic space group P-1. The structure of complex 1 consists of Keggin cluster anion  $[\text{SiW}_{12}\text{O}_{40}]^{4-}$  and charge balancing cation  $[\text{Fe}(2,2'\text{-bpy})_3]^{2+}$ . At the center of the  $[\text{SiW}_{12}\text{O}_{40}]^{4-}$  anion, the  $\text{SiO}_4$  tetrahedron is disordered over two positions related by an inversion center at the site of Si atom (Si–O distances are in the range of 1.46(1)–1.77(1) Å). The classic  $[\text{SiW}_{12}\text{O}_{40}]^{4-}$  Keggin cluster ion consists of twelve  $\text{WO}_6$  octahedra with the three types of W–O bond lengths in normal range [12]. As usual, the W–O bond lengths decrease with the decreasing coordination number of the oxygen atom, with values averaging 2.389(2) Å for four coordination ( $\text{O}_{\mu 4}$ ), 1.869(7) Å for two coordination ( $\text{O}_{\mu 2}$ ) and 1.644(4) Å for the terminal oxygen atoms ( $\text{O}_t$ ) (Table-2). Bond valence sum calculations indicate all W atoms have the oxidation number  $6^+$ . From the variations of Si–O, W–O distances and the bond angles around the Si and W atoms it is evident that there is considerable distortion in the  $\text{SiO}_4$  tetrahedra and  $\text{WO}_6$  octahedra in the complexes. This is consistent with structural features of polyoxotungstates exhibiting Keggin structures. Even though there are no “classical hydrogen bonds” between the  $[\text{Fe}(2,2'\text{-bpy})_3]^{2+}$  cations and the Keggin ion  $[\text{SiW}_{12}\text{O}_{40}]^{4-}$  anion in compound 1, there are several CH...O contacts in the range 2.28–2.60 Å between these units (Table 3). These interactions involve both terminal and bridged oxo groups of Keggin ions. Each  $[\text{SiW}_{12}\text{O}_{40}]^{4-}$  anion is hydrogen bonded to eight  $[\text{Fe}(2,2'\text{-bpy})_3]^{2+}$  cations, and in turn each  $[\text{Fe}(2,2'\text{-bpy})_3]^{2+}$  cation is hydrogen bonded to four  $[\text{SiW}_{12}\text{O}_{40}]^{4-}$  anions to form a three-dimensional network. The unit cell depicts the one formula unit of the complex where two  $[\text{Fe}(2,2'\text{-bpy})_3]^{2+}$  cations counter balance the large  $[\text{SiW}_{12}\text{O}_{40}]^{4-}$  polyanion as mentioned in combined ball-stick and ortep view of the complex (Fig1a). Besides, pictorial representation of packing diagram with ball and stick model and overall hydrogen bonded molecular structure are also given below (Fig1b,1c) for better understanding.

**Table 2: List of bond distances in complex 1**

|                   |                   |
|-------------------|-------------------|
| W–O <sub>t</sub>  | 1.626(5)–1.664(1) |
| W–O <sub>μ2</sub> | 1.767(8)–1.971(6) |
| W–O <sub>μ4</sub> | 2.191(5)–2.586(6) |
| Si–O              | 1.464(7)–1.766(5) |
| Fe(1)–N(1)        | 2.32(4)           |
| Fe(1)–N(2)        | 2.25(4)           |
| Fe(1)–N(3)        | 2.36(8)           |
| Fe(1)–N(4)        | 2.21(3)           |
| Fe(1)–N(5)        | 2.18(2)           |
| Fe(1)–N(6)        | 2.23(1)           |

**Table 3. Atomic distance (Å) and angles (°) of O<sub>POM</sub> ... H<sub>pyr</sub> interactions in the crystal structure of compound 1.**

| Donor...H...Acceptor  | d(D...H) | d(H...A) | d(D...A) | ∠DHA |
|-----------------------|----------|----------|----------|------|
| C(9)...H(9)...O(2)    | 0.94     | 2.60     | 3.34(5)  | 137° |
| C(24)...H(24)...O(5)  | 0.93     | 2.28     | 3.19(5)  | 165° |
| C(27)...H(27)...O(22) | 0.93     | 2.41     | 3.26(5)  | 153° |
| C(31)...H(31)...O(12) | 0.93     | 2.53     | 3.38(7)  | 153° |

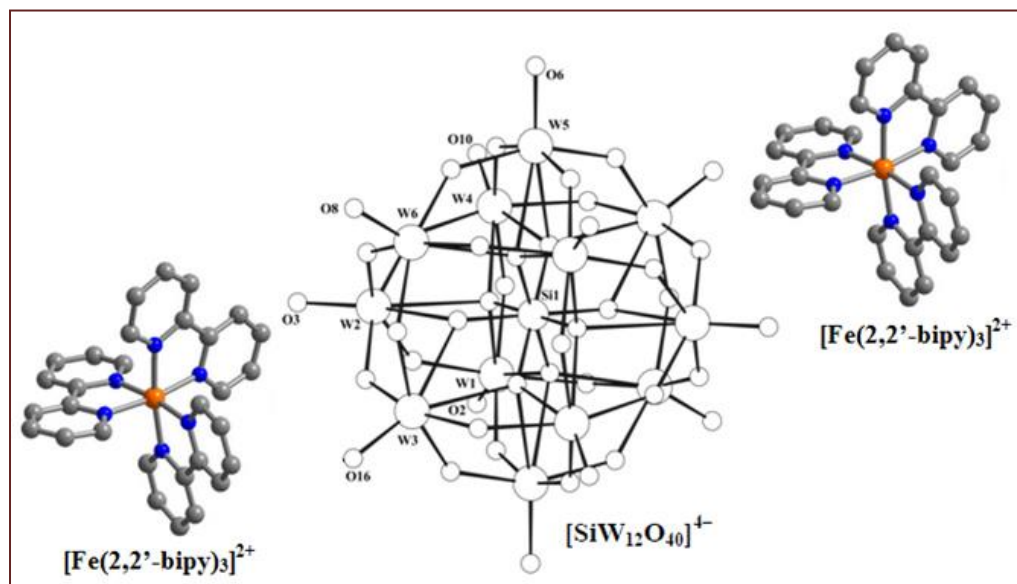


Fig.1a. Combined ball-stick and Ortep view of one formula unit of  $[\text{Fe}(2,2'\text{-bipy})_3]_2[\text{SiW}_{12}\text{O}_{40}]$

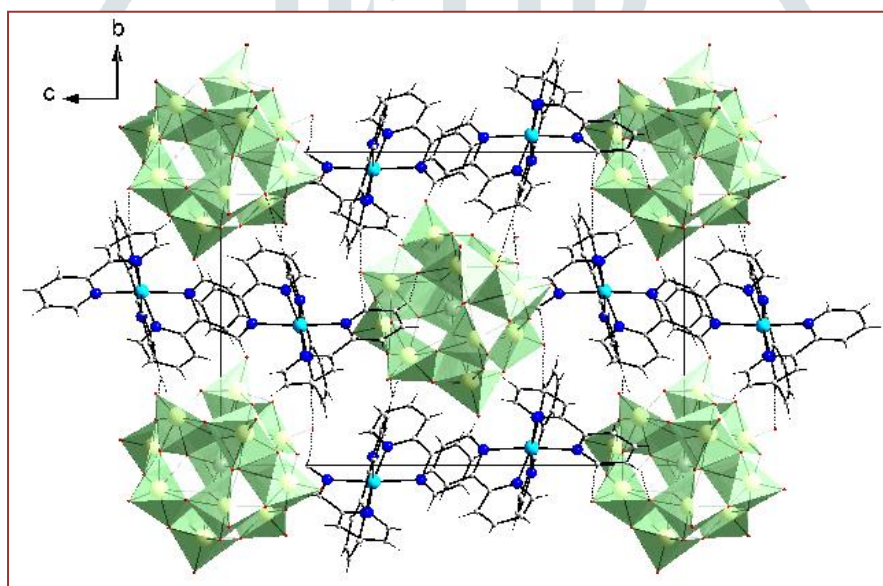


Fig.1b. Packing diagram of combined polyhedral and ball and stick model of  $[\text{Fe}(2,2'\text{-bipy})_3]_2[\text{SiW}_{12}\text{O}_{40}]$  viewed along a-axis.

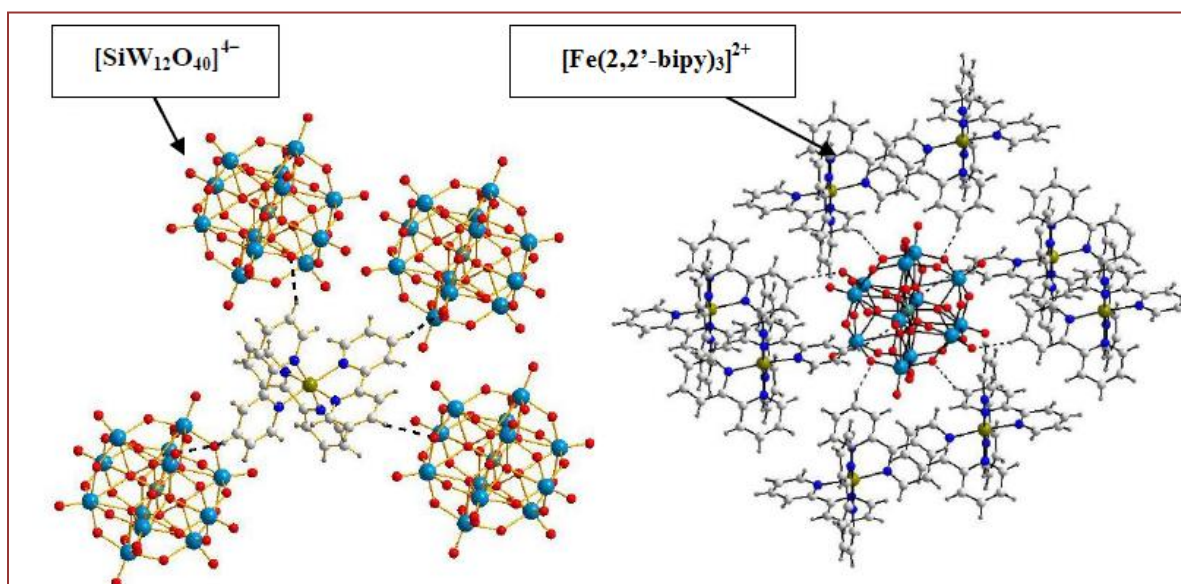


Fig. 1c. The  $[\text{Fe}(2,2'\text{-bipy})_3]^{2+}$  cation linked to  $[\text{SiW}_{12}\text{O}_{40}]^{4-}$  anions through hydrogen bonding.

The phase purity of compound 1 was confirmed by comparing the powder X-ray diffraction (PXRD) patterns of the pristine sample and the simulated pattern from the crystal structure. Purity of compound 1 was confirmed based on the basis of agreement of their PXRD diffraction patterns and the simulated patterns. (Fig.2)

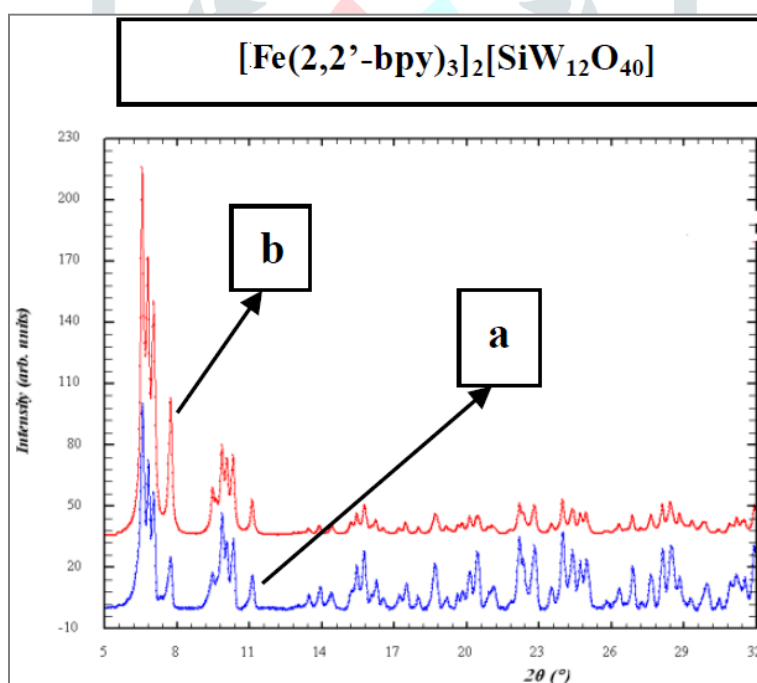
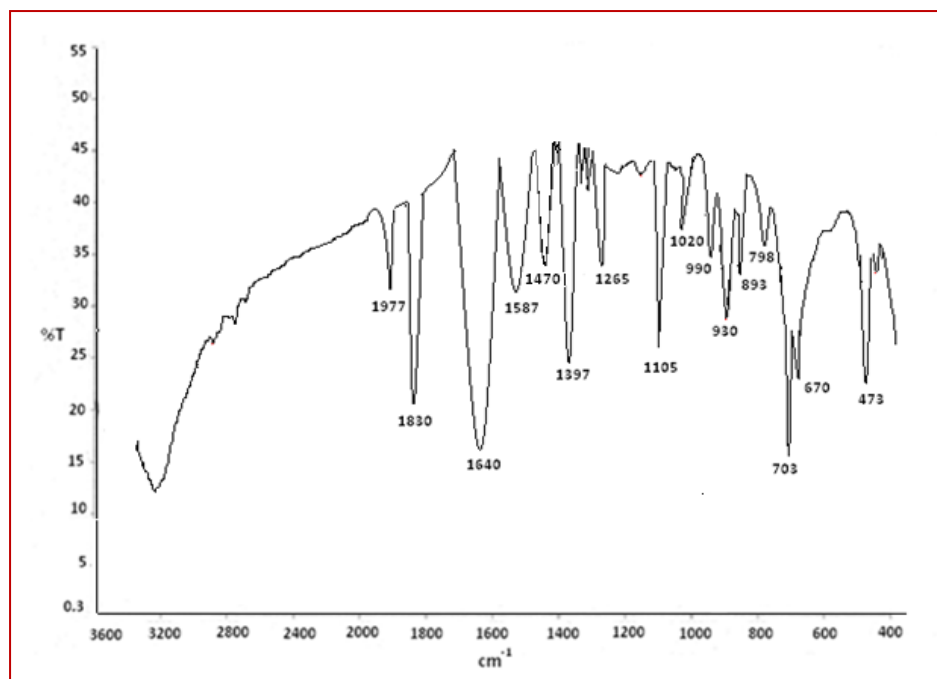


Fig.2. The powder X-ray diffraction patterns (blue line, a) and the simulated patterns (red line, b) of compound 1

## Results and discussion

### Vibrational and UV-vis spectra



**Fig.3. FTIR spectrum of complex 1, taken as KBr pellet**

For better reasoning of IR spectral values, Keggin anion  $[\text{SiW}_{12}\text{O}_{40}]^{4-}$  needs a further elucidation. The oxygen atoms in the Keggin fragment of complex 1 can be classified into three groups i.e. the unshared or terminal O atoms 'O<sub>t</sub>', the bridging O atoms (O<sub>b</sub>) connecting two W atoms, and the O atoms (O<sub>c</sub>) of the central SiO<sub>4</sub> moiety. The IR spectra of the compound (1) gives the characteristic peaks of Keggin anion at 930, 893, 798, and 703 cm<sup>-1</sup> which are attributed to  $\nu(\text{W}-\text{O}_t)$ ,  $\nu(\text{Si}-\text{O}_a)$ ,  $\nu(\text{W}-\text{O}_b)$  and  $\nu(\text{W}-\text{O}_c)$  respectively. The higher energies for the W–O and Si–O stretches are consistent with a strong interaction existing between POM anion with iron-bipyridyl cationic complex. This hybrid complex also exhibits a band about 3200 cm<sup>-1</sup>, which is the characteristic absorption of aromatic C–H stretch vibration of the 2,2'-bipyridine ligand. In addition, bands at 1587, 1470, 1397 and 1265 cm<sup>-1</sup> are assigned to characteristic vibrations of 2,2'-bipyridine. The bands at 1105, 1020 and 990 cm<sup>-1</sup> can be ascribed to the vibration of Si–O. The bands at 893 and 798 cm<sup>-1</sup> are ascribed to the vibration of W=O and W–O–W, respectively. The bands at 1640, 1587, 1397 and 1265 cm<sup>-1</sup> can specifically be assigned to the bending vibrations of OH, CH, NH, or the ring stretching frequency of the bipy ligands. The peaks near 3500 cm<sup>-1</sup> are ascribed to the stretching vibration of  $\nu(\text{O}-\text{H})$  which indicates the presence of lattice water (Fig-3). The optical absorption spectrum of compound 1 was characterized by a broad band in the visible domain around 445 nm and a band peaking at 270 nm. The visible absorption band is attributed to a metal-to-ligand charge transfer (MLCT) transition in which an electron located in a metal-based d orbital is promoted into a ligand-centered  $\pi^*$  orbital [13]. The UV absorption band corresponds to a ligand-centered  $\pi-\pi^*$  transition of 2,2'-bpy ligand, which is overlapped with the band of ligand-to-metal charge-transfer (LMCT) transitions for W(VI) (O→W).

### Thermo gravimetric analysis

The thermal stability of compounds 1 was investigated on powder samples in an air atmosphere in the temperature range 30-700°C. The TG plot (Fig-4) of compound 1 shows a weight loss of 1.25% from 30 to 200°C, which is attributed to the loss of adsorbed moisture. The weight loss of 23 to 24% in the temperature range 250-600°C corresponds to the decomposition of 2,2'-bpy ligand molecules (calculated 23.14%).

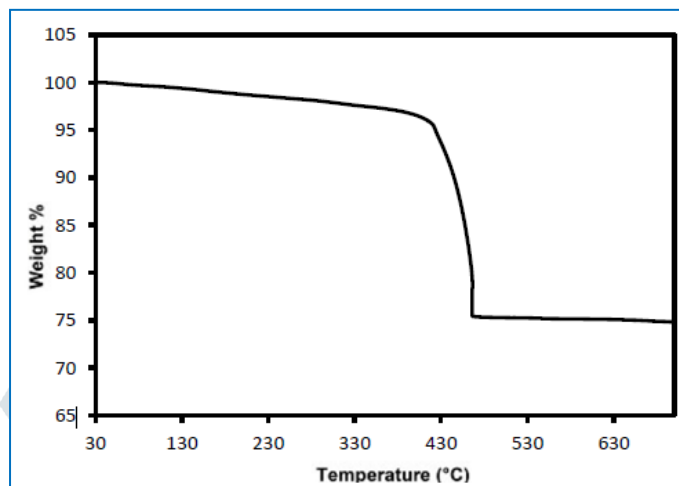


Fig.4. Thermo gravimetric analysis and weight loss profile of complex 1

### Conclusion

In summary, a new inorganic-organic hybrid based on the Keggin ion  $[\text{SiW}_{12}\text{O}_{40}]^{4-}$  was prepared hydrothermally. In this research paper, the synthesis, structure and properties of hybrid solid materials containing iron-bipyridyl complex and polyoxometalate anion have been described. Till date, Mn and Cu-bipyridyl hybrid POM have been successfully synthesized and characterized [14]. The successful isolation of compound 1 demonstrates that the hydrothermal method can also be used for the incorporation of a stable cationic complex like Fe (II)-bipyridyl into solid compounds through an electrostatic interaction to form hybrid materials. The non-covalent interactions play an important role in the assembly of the building blocks into solids which in turn direct the arrangement of these building units in the 3D space and the formation of 3D structures. There is an increasing interest and need to develop a deeper understanding of the 3D nature and behavior of organic-inorganic hybrid in chemistry. This is driven by the increased use of engineered hybrid POM and the increased pressure to commercialize this growing technology. Chatterjee et al [15] in this regard tried new crystal engineering in accordance to POM chemistry. Keeping in mind the greener side of technology, in this research article, we want to emphasize on a new synthetic methodology of the basic one-pot synthesis of polyoxometalate via acid condensation reaction. In short, I have successfully constructed organic-inorganic hybrid by grafting POM with a metal-organic frame work.

### References

- [1] Patel A., Narkhede N., Singh S., Pathan S. (2016): *Catal. Rev.* 58: 337–370.
- [2] Sambrook M.R., Notman S. (2013): *Chem. Soc. Rev.* 42: 9251–9267.



- [3] Richter M.M. (2004): *Chem. Rev.* 104(6): 3003-3006.
- [4] Sun L., Akermark B., Ott S. (2005): *Coordination Chemistry Reviews.* 249: 1653-1663.
- [5] Proust A., Matt B., Izzet G. (2012): *Chem. Soc. Rev.* 41: 7605
- [6] Kalyani V., Satyanarayana V.S., Singh V., Ghosh S. (2015) *Chem. Eur. J.* 21: 2250–2258.
- [7] Keggin J.F. (1934): *Proceedings of the Royal Society of London. Series A* 144: 75-100.
- [8] Azcarate I., Huo Z., Goldmann M., Hasenknopf B. (2015) *Chem. Eur. J.* 21: 8271.
- [9] Dolbecq A., Dumas E., Mayer C.R., Mialane P. (2014): *Chem. Rev.* 110: 6009-6048.
- [10] Ginsberg A.P. (Editor in Chief) (1990): *Inorganic synthesis*, Wiley, 27:87.
- [11] Sheldrick G.M (1998) SHELXTL PLUS. PC Version. A.
- [12] Keggin, J.F. (1933): *Nature* 131: 908-909.
- [13] Li J., Güttinger R., Moré R., Song, F. (2017): *Chem. Soc. Rev.* 46: 6124–6147.
- [14] Chatterjee R., Drew M.G.B. (2009): *Trans Met Chem.* 34(1):1-5.
- [15] Chatterjee R., Hazra D. (2014): *Polyhedron* 68: 265–271.

